Supplementary Information

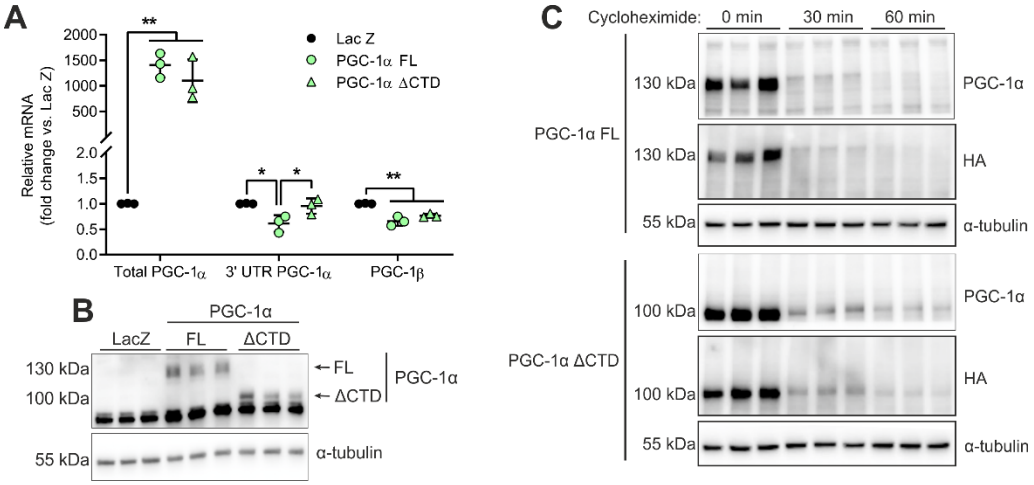

Fig. S1. Overexpression of PGC-1α FL and ΔCTD in C2C12 myotubes. (A, B) PGC-1α mRNA (A) and protein (B) levels in C2C12 myotubes transduced with LacZ (control), PGC-1α FL or ΔCTD (n = 3 independent experiments each in triplicate). (C) PGC-1α protein half-life analysis in C2C12 myotubes transduced with PGC-1α FL or ΔCTD and treated with DMSO as control or 100 μg/ml cycloheximide. Values are mean ± SD; *$p < 0.05$ and **$p < 0.01$. Immunoblots are representative of three independent experiments, each performed in triplicate.

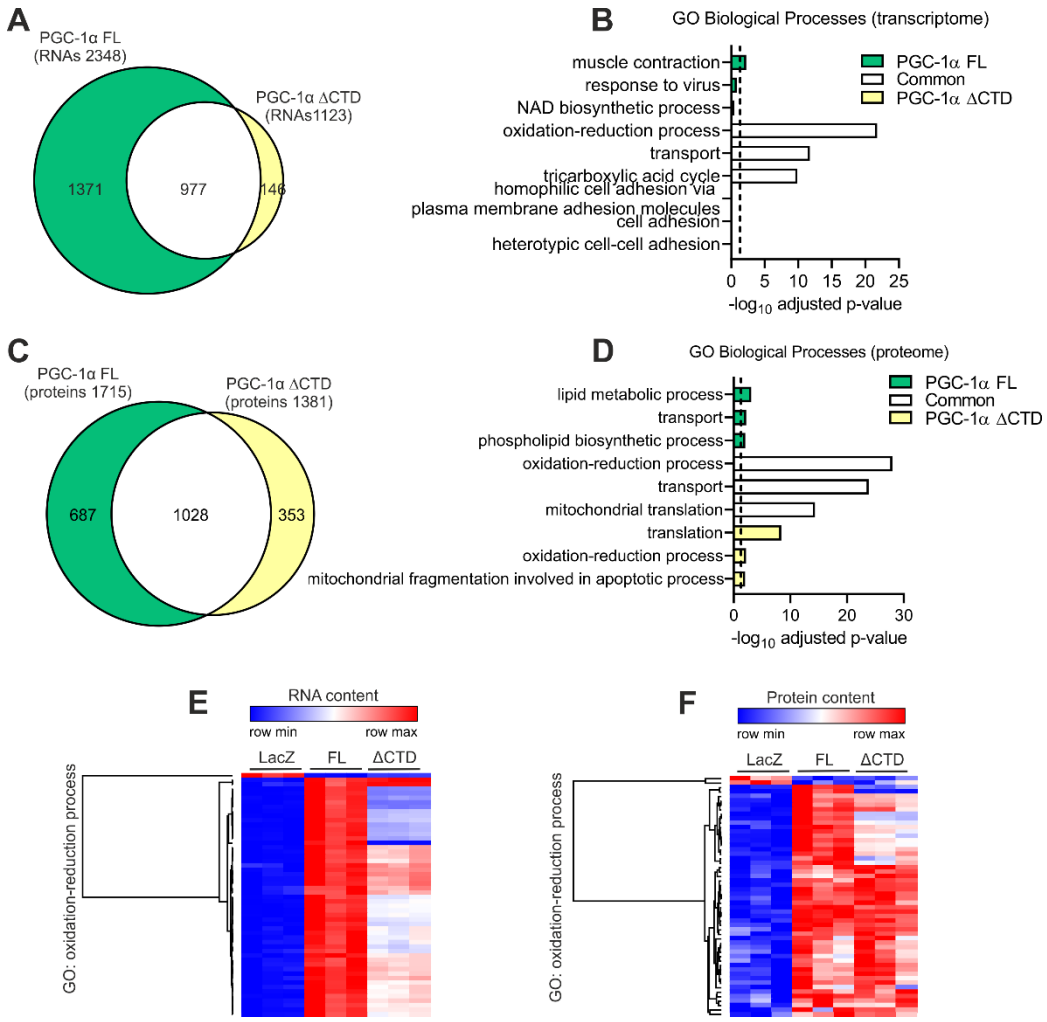

Fig. S2. Transcriptome and proteome analysis. (A, B) Overlap (A) and gene ontology (GO) analysis (B) of DEG induced by PGC-1α FL or ΔCTD in C2C12 myotubes. (C, D) Overlap (C) and GO analysis (D) of proteins regulated by PGC-1α FL or ΔCTD in C2C12 myotubes. (E, F) Heat maps showing the content of RNAs (E) and proteins (F) contained in the GO term oxidation-reduction process in C2C12 myotubes overexpressing LacZ (control), PGC-1α FL or ΔCTD. Dashed line represents GO statistical cutoff (adjusted p-value < 0.05).

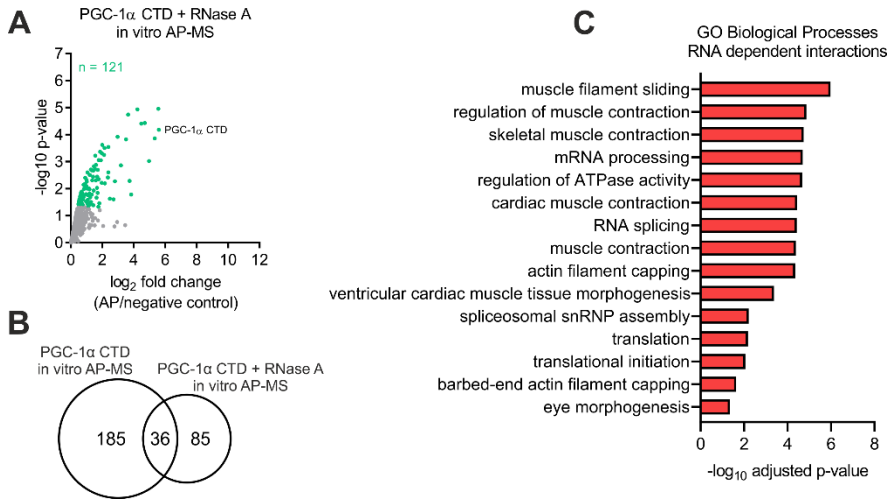

Fig. S3. RNA dependent protein-protein interaction analysis. (A) Volcano plot with green dots representing proteins interacting with the CTD of PGC-1α in the presence of 1 mg/ml of RNase A. (B) Overlap of PGC-1α CTD interacting proteins in the absence and presence of 1 mg/ml of RNase A. (C) Gene ontology (GO) analysis of RNA dependent PGC-1α CTD interacting proteins.

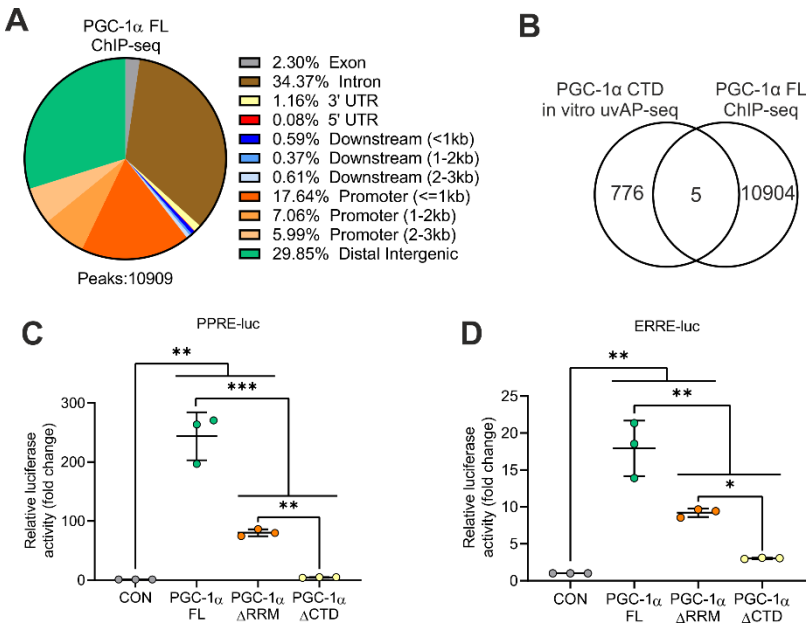

Fig. S4. ChIP-seq analysis of PGC-1α FL and reporter gene assay. (A) Annotation of PGC-1α FL ChIP-seq peaks. (B) Overlap of PGC-1α CTD and FL in vitro AP-seq and ChIP-seq peaks, respectively. (C and D) Relative luciferase activity of PPRE-luc (C) and ERRE-luc (D) reporter plasmids in HEK293 cells co-transfected with PPARβ/δ (PPRE-luc) or ERRα (ERRE-luc) in the absence (CON: control) and presence of PGC-1α FL, ΔRRM or ΔCTD (n = 3 independent experiments, each performed in triplicate). Values are mean ± SD; *$p < 0.05$, **$p < 0.01$ and ***$p < 0.001$.

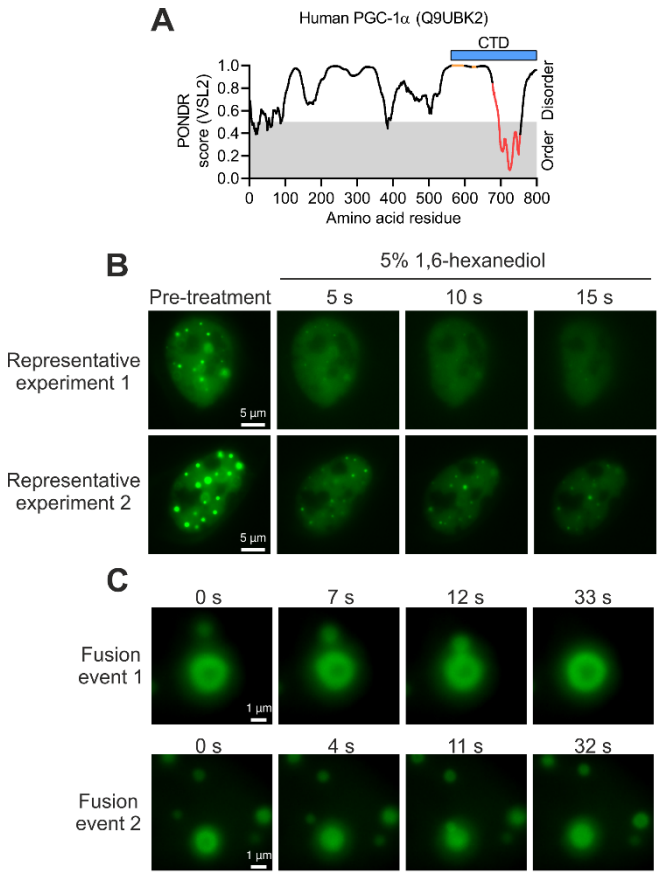

Fig. S5. Analysis of liquid-like properties of PGC-1α nuclear foci. (A) Predictor of Natural Disordered Regions (PONDR) analysis of human PGC-1α protein, with orange and red dots representing RS domains and RRM, respectively. (B) Additional live imaging of 5% 1,6-hexanediol treatment of C2C12 myoblasts transfected with GFP-PGC-1α FL. (C) Additional live imaging of GFP-PGC-1α FL droplet fusion events in C2C12 myoblasts. Microscopy images are representative of at least three independent experiments, each performed in triplicate.

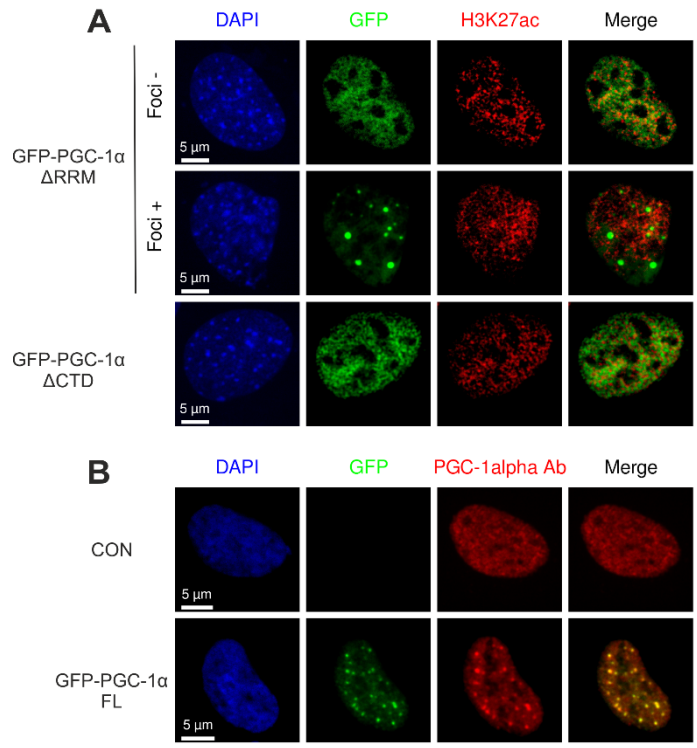

Fig. S6. PGC-1α nuclear condensates and immunofluorescence staining. (A) Images of transfected GFP-PGC-1α ΔRRM or ΔCTD co-stained with DAPI and H3K27ac in C2C12 myoblasts. (B) Images of HEK293 cells transfected with a control (CON) empty plasmids or GFP-PGC-1α FL co-stained with DAPI and PGC-1α antibody (Ab). Microscopy images are representative of at least three independent experiments, each performed in triplicate.

Movie S1. Fusion of PGC-1α nuclear condensates. Representative movie of GFP-PGC-1α FL droplet fusion in C2C12 myoblasts.